DOI: 10.1002/ejoc.201200985

Atropisomeric Chiral Probes to Study the Supramolecular Organization in Porphyrin Self-Assemblies

Cyril Chappaz-Gillot,[a] Gabriel Canard,*[a] Federico Andreoli,[a] Nicolas Vanthuyne,[a] Michel Giorgi,[b] Jean-Valère Naubron,[b] Valérie Monnier,[b] Roselyne Rosas,[b] Christian Roussel,[a] and Teodor Silviu Balaban[a]

Keywords: Porphyrinoids / Self-assembly / Chirality / Circular dichroism / Aggregation

A noncatalysed nucleophilic aromatic substitution was used to prepare the (bacterio)chlorophyll mimics **2**-Zn, **3**-Zn, **4**-Zn and **5**-Zn. The localisation of the two recognition groups on the same side of the porphyrin macrocycles in **2**-Zn, **4**-Zn and **5**-Zn produces, through metal–ligand interactions, oligomers that display both H- and J-type aggregates. These supramolecular architectures were confirmed by the introduction of optically pure atropisomers in **5**-Zn, which produces chiral aggregates. The UV/Vis and electronic circular dichroism spectra of all aggregates are used to propose an excitonic splitting mode that would correspond to this dual type of chromophoric self-assembly.

Introduction

Chromophoric self-assemblies are of particular interest in the design of materials for excitation energy transfer and electron-hole transport systems. The supramolecular organisation of monomers allows the π-electronic systems to overlap and interact to produce assemblies showing new functions that are not observed in the corresponding monomers. Usually the UV/Vis spectra of such aggregates feature a regular arrangement of chromophores through excitonic couplings that expand the resulting light absorption, which is crucial for constructing efficient light-harvesting systems. These properties are directly linked to the supramolecular organisation of the chromophores, which controls their orientation and orbital overlap. When no single-crystal X-ray diffraction data are available to accurately characterise these assemblies, one has to use and interpret complex spectroscopic features to ascribe a proposed model of organisation. Consequently, there is still a need for complementary tools to determine the spatial arrangement of chromophores and thereby explain the resulting electronic and spectroscopic properties.

Porphyrins are one of the most studied tectons that have been incorporated into large assemblies, because their chemical structure resembles that of (bacterio)chlorophylls, which build well-defined superstructures in natural light-harvesting systems such as light-harvesting complexes (LH1, LH2) or chlorosomes.[1] Different types of organisation can describe the porphyrin self-assemblies, which produce H- (face-to-face), J- (head-to-tail) or both H- and J- (slipped cofacial) type aggregates.[2] When two porphyrins interact, the first set of transition dipoles B_x and B_y produces excitonic couplings, resulting in a blueshift (H-dimer), redshift (J-dimer) or splitting (slipped cofacial dimer) of the former degenerate monomer Soret band. Consequently, the UV/Vis spectra of large assemblies containing mixed aggregate types are generally difficult to interpret due to the overlap of multiple absorption bands and due to the combination of multiple excitonic couplings.

We have studied zinc porphyrin **1**-Zn as a (bacterio)-chlorophyll mimic that produces organised light-harvesting self-assemblies (Scheme 1).[3] This compound bears a hydroxyethyl and a carbonyl group that coordinate the zinc ion in a 5½ fashion that is responsible for the organisation of the (bacterio)chlorophyll aggregates.[4] The localisation of these two recognition groups on opposite sides of the

[a] Aix-Marseille Université, CNRS-UMR 7313 – Institut des Sciences Moléculaires de Marseille (ISM2) – Chirosciences, Faculté des Sciences de Saint-Jérôme Case A62, Avenue Escadrille Normandie Niemen, 13397 Marseille, Cedex 20, France
Fax: +33-4-91289146
E-mail: gabriel.canard@univ-amu.fr
Homepage: www.ism2.univ-cezanne.fr
[b] Aix-Marseille Université, FR 1739 - Fédération des Sciences Chimiques de Marseille – Spectropole, Faculté des Sciences de Saint-Jérôme Case A62, Avenue Escadrille Normandie Niemen, 13397 Marseille, Cedex 20, France

Supporting information for this article is available on the WWW under http://dx.doi.org/10.1002/ejoc.201200985.

porphyrin macrocycle allows the supramolecular organisation of well-defined J-aggregates in which each zinc ion of one porphyrin interacts with the hydroxyethyl group of another porphyrin and the carbonyl group of a third. In the search for new kinds of supramolecular organisations that display original spectroscopic features, we designed zinc porphyrin **2**-Zn (Scheme 1). Compared with **1**-Zn, **2**-Zn has its two recognition groups, the nitrogen NH on the porphyrin and the oxygen of an urea, located on the same side of the porphyrin macrocycle.

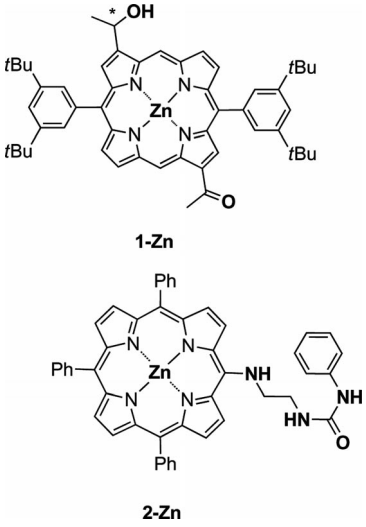

Scheme 1. Chemical groups involved in supramolecular interactions are printed in bold.

We describe here the synthesis and self-assemblies of four simple (bacterio)chlorophyll mimics bearing one or two recognition groups introduced on the same side of the porphyrin core. The incorporation of an atropisomer as an original chiral element induces a supramolecular chirality that allows the use of electronic circular dichroism (ECD) spectra to deconvolute complex UV/Vis spectra of multiporphyrinic assemblies. The spectroscopic data were used to propose a new supramolecular packing that displays both J- and H-type aggregation.

Results and Discussion

Synthesis

We described recently the introduction of various amines on the porphyrin core by an noncatalysed nucleophilic aromatic substitution.[5] This procedure was here used to introduce the recognition groups of the (bacterio)chlorophyll mimics (Scheme 2). For example, when an excess of propylamine was added to the *meso*-bromoporphyrin **6**, porphyrin **3**-2H was produced in less than 24 hours in good yield. A small volume of tetrahydrofuran was introduced as a cosolvent because compound **6** was not soluble in propylamine. Porphyrin **3**-2H bears only the NH functional group and its structure was ascertained by X-ray single-crystal diffraction (Figure S1 in the Supporting Information). When propylamine was replaced by ethylenediamine, the same procedure produced **4**-2H, which brings an additional amino NH_2 recognition group. This functional group offers numerous possibilities of further functionalisations. The condensation of phenyl isocyanate on **4**-2H afforded porphyrin **2**-2H quantitatively, in which the two recognition groups are the *meso*-NH on the porphyrin and the carbonyl group of a urea. Furthermore, the NH moieties of the urea can be involved in additional hydrogen-bonding interactions. The introduction of a chiral element was achieved through replacement of the phenyl ring of the urea of **2**-Zn by an optically pure *N*-phenyl-substituted thiazolinethione atropisomer (Scheme 2).[6] The racemic mixture was also prepared to assess the impact of the optical purity on the supramolecular organisation. The isocyanate derivatives (*rac*)-**8**, (*aR*)-**8** and (*aS*)-**8** were prepared in situ by reacting *N*-(2-aminophenyl)-4-methylthiazoline-2-thiones (*rac*)-**7**, (*aR*)-**7** and (*aS*)-**7** with triphosgene. These isocyanates were added to a solution of **4**-2H and afforded quantitatively the free base porphyrins (*rac*)-**5**-2H, (*aR*)-**5**-2H and (*aS*)-**5**-2H. Because of the strong absorbance of porphyrins in the UV/Vis domain, it was not possible to record rotatory power on conventional polarimeters. Consequently, the optical purities of (*aS*)-**5**-2H and (*aR*)-**5**-2H were analyzed by analytical chiral HPLC after their synthesis to confirm that no racemisation had occurred. First, the racemic compound (*rac*)-**5**-2H was subjected to chiral HPLC analysis to establish the retention times of the two atropisomers. After screening of a range of chiral stationary phases and solvents, a Chiralpak IC column was chosen together with a mixture of hexane and ethanol (80:20) as the solvent system. At 25 °C, the two atropisomers were well-separated with retention times of 16.9 and 21.9 min (Figure 1a). The same procedure was applied to analyse the optical purities of samples of (*aR*)-**5**-2H and (*aR*)-**5**-2H, which revealed no detectable racemisation (Figure 1, b and c). The absolute configurations of **5**-2H were those of optically pure **7** attributed previously.[6,7] Finally, all the free-base porphyrins were metalated by zinc acetate to generate the (bacterio)chlorophyll mimics **2**-Zn, **3**-Zn, **4**-Zn and **5**-Zn. The optical purities of the zinc complexes (*aR*)-**5**-Zn and (*aS*)-**5**-Zn could not be determined because of their strong interactions with the chiral phases. Because no racemisation occurred during the preparation of optically pure (*aR*)-**5**-2H and (*aS*)-**5**-2H and taking into account the high values of the racemisation barriers measured for thiazolinethione atropisomers (ca. 130 kJ mol^{-1}), we are confident that the conditions used for their metalation (zinc acetate, dichloromethane, methanol, room temperature) are mild enough to avoid any isomerisation.[6]

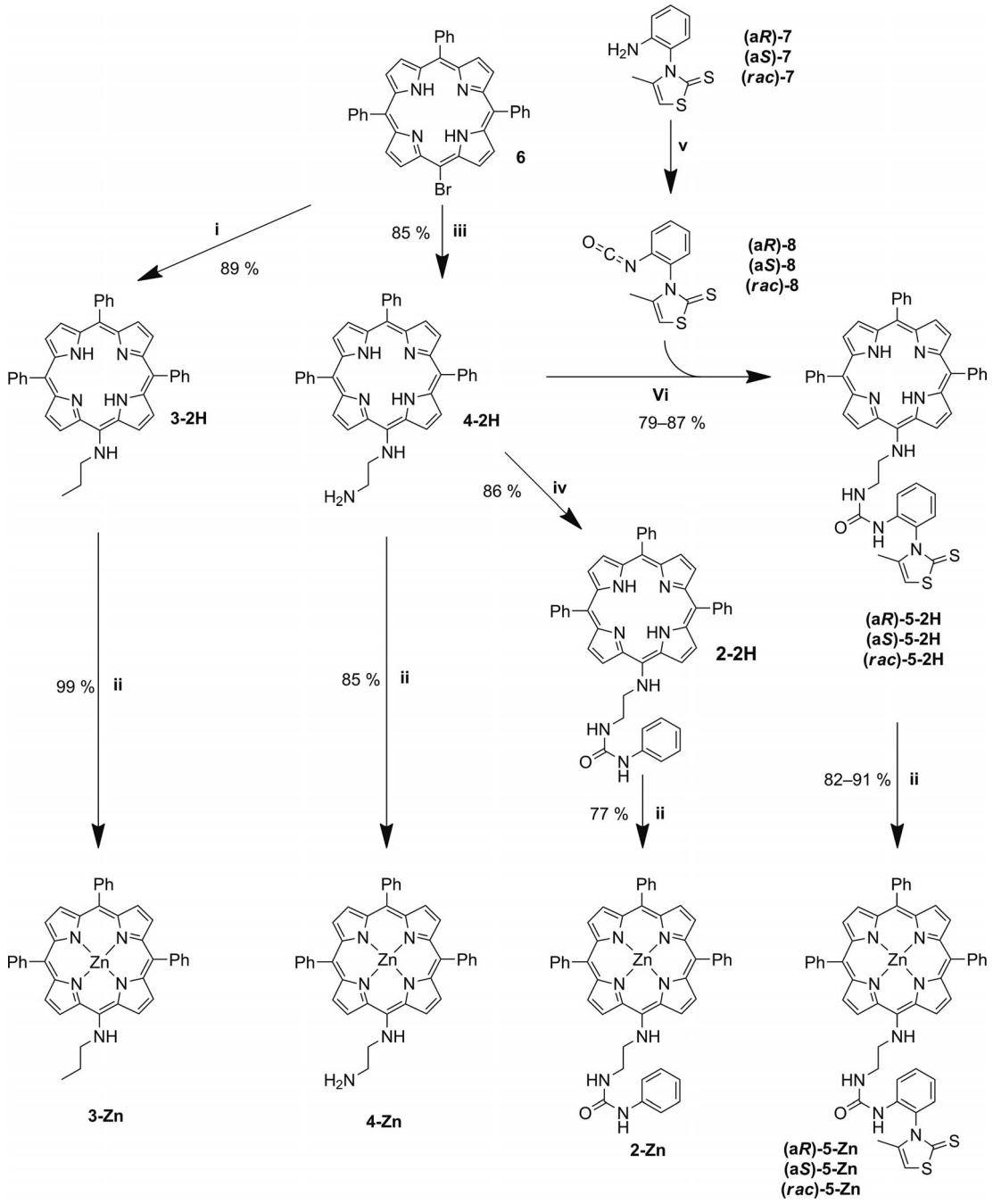

Scheme 2. (i) Propylamine, THF; (ii) $Zn(OAc)_2 \cdot 2H_2O$, CH_2Cl_2, MeOH; (iii) ethylenediamine, THF; (iv) phenyl isocyanate, CH_2Cl_2; (v) triphosgene, $(i\text{Pr})_2\text{NEt}$, CH_2Cl_2; (vi) CH_2Cl_2.

Coordination to the Zinc Porphyrin by Various Model Ligands

The aggregation of zinc porphyrins **2**-Zn, **3**-Zn, **4**-Zn and **5**-Zn in nonpolar solvents depends on various intermolecular interactions that needed to be identified. For this purpose, we chose to analyse the interaction between the zinc metallic centre of the simple zinc porphyrin **9**-Zn and model ligands that mimic the functional groups borne by compounds **2**-Zn, **3**-Zn, **4**-Zn and **5**-Zn. We selected propylamine **10**, *N*-methylaniline **11**, *N*,*N*′-dimethylurea **12** and thiazolinethione **13** and studied by UV/Vis spectroscopy their ability to coordinate zinc porphyrin **9**-Zn (Scheme 3).

The model ligand (ca. 10–15 equiv.) was dissolved in 3 mL of a solution of zinc-porphyrin **9**-Zn (1.4 mg) in dichloromethane (100 mL). The resulting solution was transferred to a UV quartz cuvette with a 1 cm pathlength and the UV/Vis spectrum was recorded from 400 to 800 nm. The maxima of the Soret and the Q bands and their redshift values were compared to the maxima of the

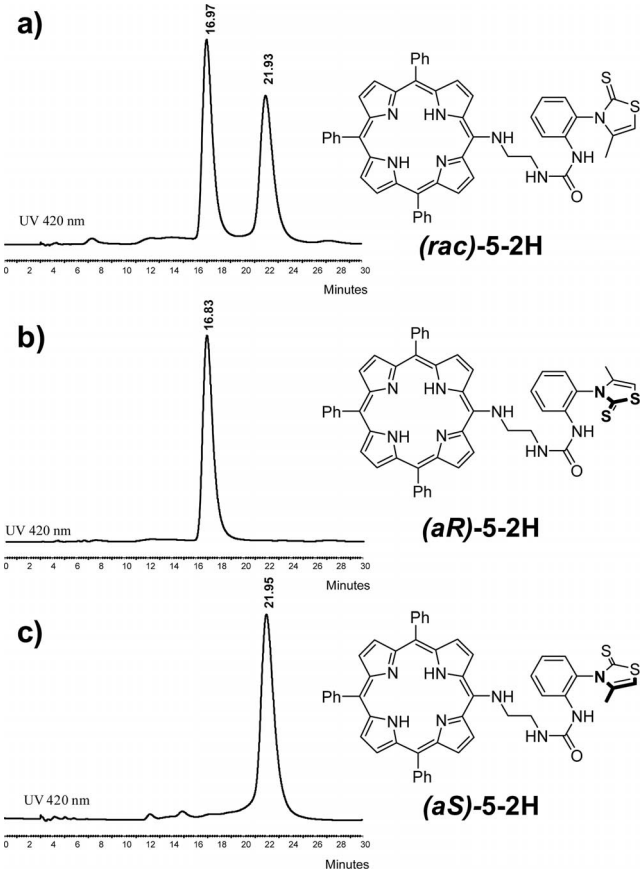

Figure 1. Chromatograms (UV/Vis detection) of the chiral HPLC analysis of the two atropisomers of (a) (*rac*)-**5**-2H, (b) (*aR*)-**5**-2H and (c) (*aS*)-**5**-2H.

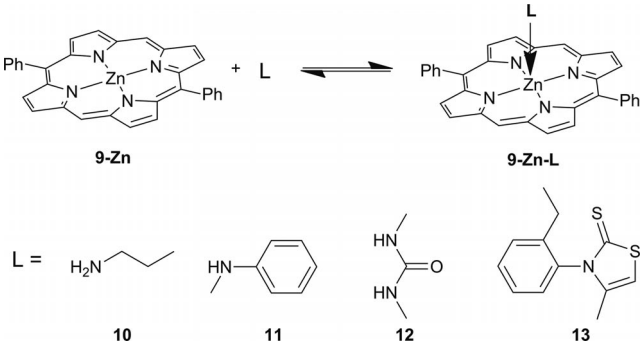

Scheme 3. Coordination of the model ligands **10**, **11**, **12** and **13** by zinc porphyrin **9**-Zn.

reference zinc porphyrin **9**-Zn (Table 1). If no changes in the wavelength of the maxima were observed, the **L**/**9**-Zn ratio was raised to reach 150. Propylamine **10** and *N*-methylaniline **11** interact strongly with **9**-Zn and produced significant redshifts of the Soret and Q bands. The coordination of *N*,*N*′-dimethylurea **12** was much weaker and could be visualised only by adding a large excess of the ligand; no interaction occurred between the thiazolinethione **13** and **9**-Zn despite the application of a very large **L**/**9**-Zn ratio. This study shows that the aggregation of porphyrins **2**-Zn, **3**-Zn, **4**-Zn and **5**-Zn are based on the ligation of the zinc ion by three different ligands: the *meso*-NH group of the porphyrin, the terminal amino group or the carbonyl of the urea. The chiral thiazolinethione fragment introduced in **5**-Zn is inert and does not afford a supplementary zinc–ligand interaction compared to **2**-Zn.

Table 1. Maxima of the UV/Vis spectra of the complexes **9**-Zn**/L**.

Ligand **L**	Ratio L/**9**-Zn	UV/Vis, λ_{max} ($\Delta\lambda$)[a] [nm] Soret	Q
None	0	409 (0)	538 (0), 571 (0)
Propylamine **10**	15	417 (8)	551 (13), 588 (17)
N-Methylaniline **11**	12	417 (8)	547 (9), 584 (13)
N,*N*′-Dimethylurea **12**	150	414 (5)	544 (6), 581 (10)
Thiazolinethione **13**	150	409 (0)	538 (0), 571 (0)

[a] $\Delta\lambda$ is the redshift observed (nm) during the coordination process.

Self-Assembly of 2-Zn

2-Zn self-assembles in nonpolar solutions at very dilute concentrations so that only the use of strongly coordinating solvents such as dimethyl sulfoxide (DMSO) produces sharp and interpretable signals in the corresponding ^{1}H NMR spectra. Figure 2 (a) shows the UV/Vis spectrum of **2**-Zn aggregates recorded when a small volume (50 μL) of a concentrated solution of **2**-Zn in dichloromethane is diluted into larger volume of dry *n*-heptane (3 mL). The monomer **2**-Zn can be recovered by adding a few drops of methanol, which causes the gradual disassembly of aggregates due to its competition for metal ligation, forming **2**-Zn/MeOH adducts.

The self-assembly process causes a strong broadening of the Soret and Q bands. A small redshift is observed for the Q bands (566→573 nm, 612→616 nm), whereas the Soret band splits into three bands, one with a maximum at 429 nm and two flanking discernible shoulders, one blueshifted to 410 nm, and one redshifted to 450 nm. This result clearly shows that self-assembly occurs between single **2**-Zn molecules through intermolecular interactions but does not give any direct information on the supramolecular organization, which is also illustrated by the blueshifted quenched fluorescence (Figure S2 in the Supporting Information). Even if excitonic dipole–dipole theory could explain the evolution of the UV/Vis spectrum and thereby be a strong validation requirement of any proposed model,[8] other experimental evidence is necessary to evaluate the intermolecular organisation.

We were not able to obtain suitably diffracting single crystals of the **2**-Zn aggregates, so we resorted to preparing several related zinc porphyrins to study the different key roles of the functional groups in the construction of the assembly and their signatures in the UV/Vis spectra of the aggregates. Consequently, the simpler complexes **3**-Zn and **4**-Zn were prepared (Scheme 2).

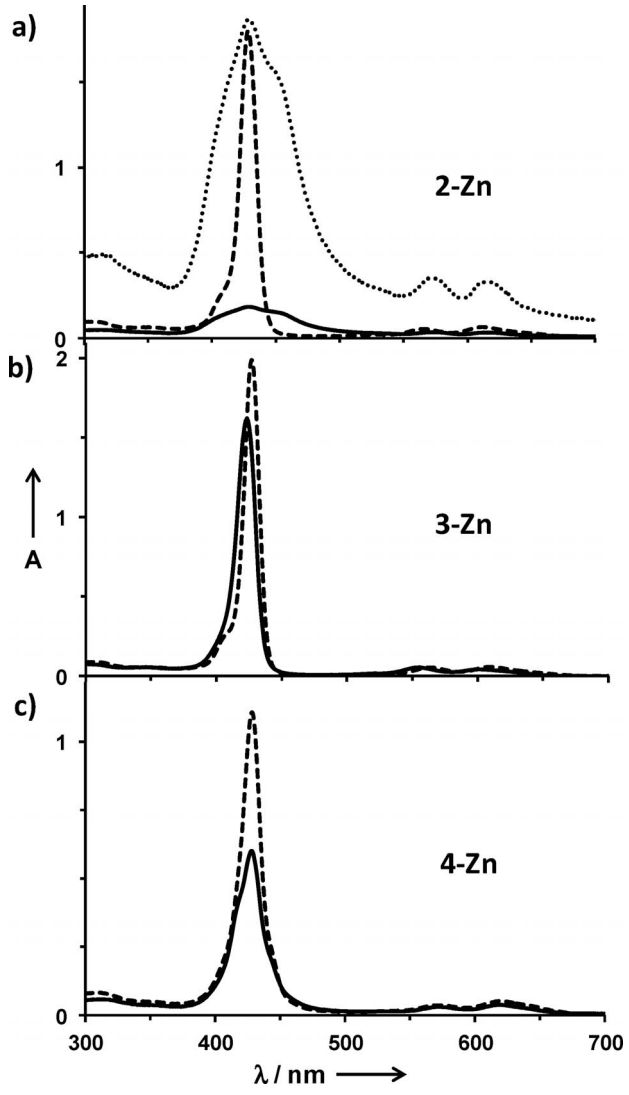

Figure 2. (a) Solid trace: dilution of a dry, concentrated dichloromethane solution of **2**-Zn in *n*-heptane. Dotted trace: same spectrum muliplied by 10. Dashed trace: the same solution after addition of methanol. (b) Solid trace: dilution of a dry, concentrated dichloromethane solution of **3**-Zn in *n*-heptane. Dashed trace: the same solution after addition of methanol. (c) Solid trace: dilution of a dry, concentrated dichloromethane solution of **4**-Zn in *n*-heptane. Dashed trace: the same solution after addition of methanol.

Self-Assembly of 3-Zn

Just as for **2**-Zn, **3**-Zn self-assembles in nonpolar solvents under very dilute conditions so that, again, only the use of strongly coordinating solvents such as DMSO produced sharp and interpretable signals in the corresponding ^{1}H NMR spectra. **3**-Zn forms H-type oligomers that are dissociated by the addition of an excess of a strong coordinating ligand such as MeOH or DMSO. The introduction of a concentrated dichloromethane solution of **3**-Zn into *n*-heptane produced aggregates that were revealed by a 6–10 nm blueshift of the Soret band (430→424 nm) and the Q bands (565→555 nm, 612→601 nm) due to the formation of H-dimers or H-trimers built on Zn–NH intermolecular interactions (Figure 2, b). As depicted in Scheme 4, the excitonic dipole–dipole coupling occurring in these oligomers affects the B_x and B_y transition dipoles producing an overall blueshift of the Soret band that is still relatively small. This blueshift is also due to the metal–ligand interaction of the **3**-Zn/MeOH adduct, which is replaced by a Zn/NH interaction. This finding shows that the NH recognition group on the porphyrin skeleton is able to interact with the zinc ion of a second porphyrin to form H-dimers, which are probably responsible for the blueshift contribution of the split Soret band observed in **2**-Zn aggregates.

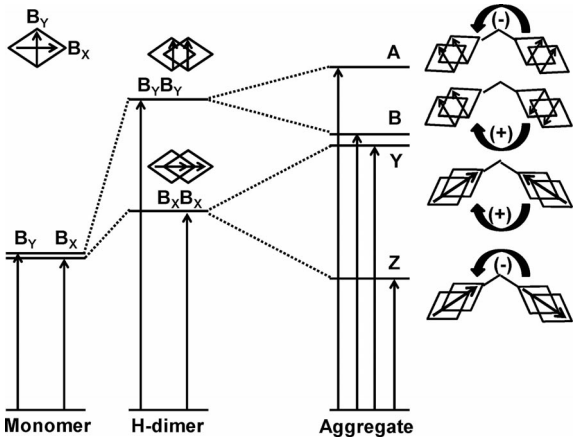

Scheme 4. Excitonic dipole–dipole coupling occurring within **2**-Zn, **4**-Zn or **5**-Zn oligomers (forbidden transitions are not shown).

Self-Assembly of 4-Zn

We also prepared porphyrin **4**-Zn, which brings an additional amino NH_2 recognition group. As mono-*ortho*-aniline-substituted zinc porphyrins,[9] **4**-Zn spontaneously forms at a micromolar scale J-dimers through two Zn–NH_2 intermolecular interactions even in a strong coordinating solvent such as DMSO. When the ^{1}H NMR spectrum of **4**-Zn was recorded at a micromolar scale in [D_6]DMSO, the signals of the terminal methylene and amino groups CH_2 and NH_2 were observed to be strongly shielded (δ = –0.59 and –1.32 ppm, Figure 3). We suspected that this could be the result of the strong dimerisation of **4**-Zn, which places a part of the alkyl chain above the porphyrin core. It should be noted that the use of a less polar solvent produces very broad signals due to aggregation of these dimers. Despite this strong evidence, one could think that this well-resolved ^{1}H NMR spectrum could be assigned to a more complex structure such as a cyclic trimer or tetramer. Therefore, a detailed mass spectrometric analysis was performed to study the formation of this dimer (Figure 4). The ESI-MS spectrum of **4**-Zn recorded in a solution of sodium chloride in methanol displays the most abundant ion of the protonated monomer (*m*/*z* 659) and its adduct with sodium (*m*/*z* 681). The two corresponding expected adducts of the dimer (*m*/*z* 1321 and 1343) can also be seen, revealing the remarkable stability of the dimer even during the ionisation process. With almost the same intensities, ions corresponding to the trimer were detected (*m*/*z* 1981 and 2003). This trimer

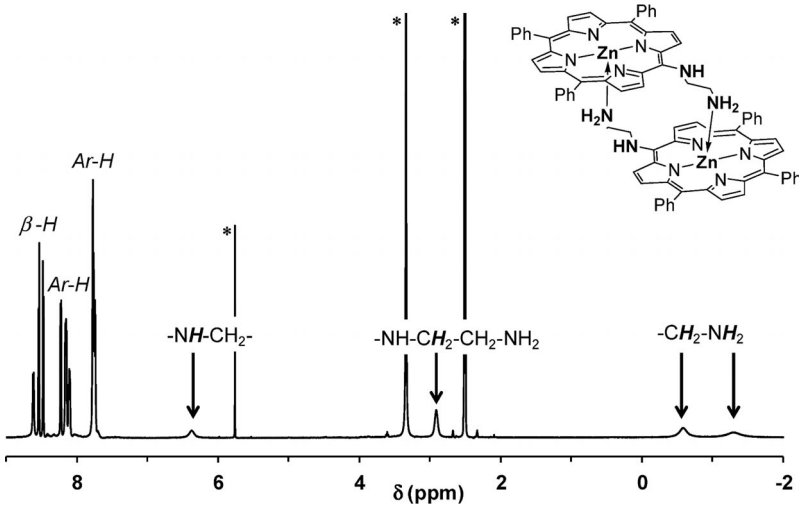

Figure 3. ^{1}H NMR (400 MHz) spectrum of **4**-Zn in [D$_6$]DMSO. Asterisks denote residual solvent peaks.

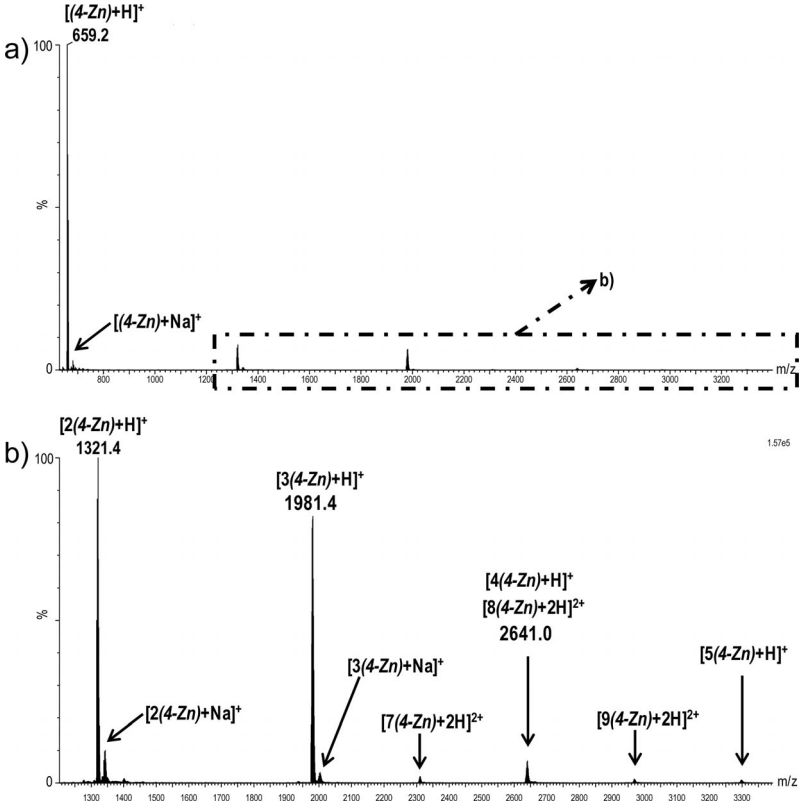

Figure 4. (a) Positive ESI-MS spectrum of **4**-Zn recorded in a solution of sodium chloride in methanol [(***4-Zn***) is the monomer]. (b) Expansion of the region in which multiple oligomers are detected.

probably results from the self-assembly of one monomer to one dimer in the gas phase. The strong self-assembly of **4**-Zn is also illustrated by less intense ions corresponding to higher oligomers. A high-resolution mass spectrometry analysis was performed on the isotopic maximum of the sodium-dimer adduct and confirmed its elementary composition (calcd. for $C_{80}H_{60}N_{12}Zn_2Na^+$ 1343.3521 [2(**4**-Zn) + Na]$^+$; found 1343.3518). DOSY NMR experiments confirmed the formation of this dimer (see the Supporting Information).

The excitonic dipole–dipole coupling occurring in this J-dimer and the strong Zn–NH_2 interactions produce a small redshift of all bands compared to the spectrum of the monomer **3**-Zn (Figure 2, b and c). The addition of *n*-hept-

ane causes a strong broadening and splitting of the Soret band with a maximum at 428 nm and two discernible shoulders at 415 and 443 nm, whereas the Q bands are slightly blueshifted (575→572 nm, 622→619 nm) (Figure 2, c). A similar change of the absorption spectrum was observed during the aggregation of **2**-Zn and reveals a supramolecular organisation that can only be explained by a new Zn–NH inter-dimer interaction producing new excitonic couplings. In the solid state, the organisation of the chromophore can then be described as a H-aggregate of J-dimers or as a J-aggregate of H-dimers (Scheme 5). When two H-dimers interact, the angles between the two transition dipoles B_XB_X or B_YB_Y are probably small and the splitting energies are weak. The splitting of the Soret band is then small and results from four permitted electronic transitions ABYZ of similar energies (Scheme 4). An identical splitting mode was used to describe hexameric macrorings of slipped-cofacial dimers.[10] The same model can be applied for the self-assembly of **2**-Zn that is based on Zn–NH and Zn–O=C intermolecular interactions (Scheme 5). When **2**-Zn or **4**-Zn are dissolved in a nonpolar solvent, the strongest metal–ligand interaction Zn–NH or Zn–NH_2 produces H- or J-dimers that assemble into higher oligomers due to secondary and weaker metal ligation Zn–O=C or Zn–NH. To confirm these hypotheses and the corresponding splitting mode, we studied the aggregation of **5**-Zn.

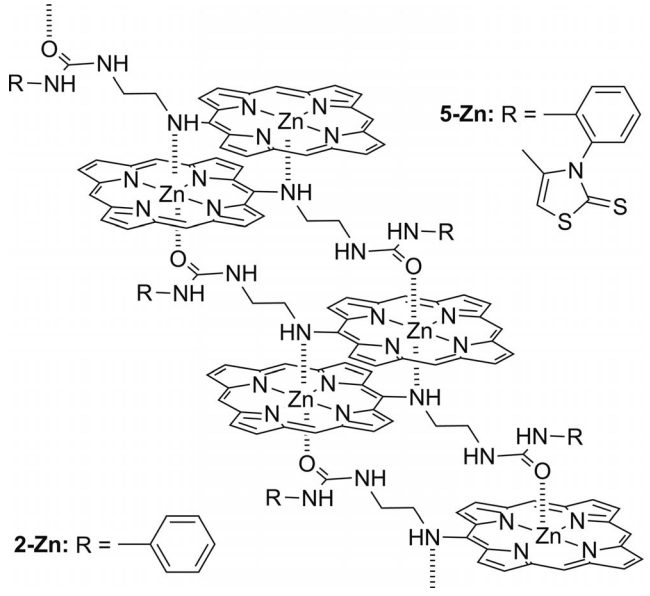

Scheme 5. Self-assemblies of zinc porphyrins **2**-Zn or **5**-Zn (*meso*-phenyl groups are omitted for clarity). The same organisation occurs during the aggregation of **4**-Zn in which the Zn–O=C intermolecular interactions are replaced by strong Zn–NH_2 interactions.

Self-Assembly of 5-Zn

ECD is a well-known technique that is used to describe the interactions of porphyrins or chromophores through space[11] and has been successfully applied to study numerous chiral assemblies.[12] This technique helped us to fully resolve the **2**-Zn supramolecular organization by inducing chirality to the aggregates. For this purpose, we prepared (*rac*)-**5**-Zn, (*aR*)-**5**-Zn and (*aS*)-**5**-Zn in which the phenyl ring of the urea of **2**-Zn is replaced either by a racemic or an optically pure *N*-phenyl-substituted-thiazolinethione atropisomer (Scheme 2).[6] A UV/Vis survey of all possible intermolecular interactions between **2**-Zn, **3**-Zn, **4**-Zn or **5**-Zn monomers showed that zinc ligation by a *N*-substituted-thiazolinethione is impossible, revealing the inertness of this supplementary introduced fragment.

The self-assembly of **5**-Zn produces spectral features that are similar to those observed for **2**-Zn. A small redshift is observed for the Q bands (561→572 nm, 613→618 nm), whereas the broad Soret band appears split with a maximum at 424 nm and two discernible shoulders at 410 and 445 nm (Figure 5, a). Another excitonic coupling affects the absorption of the thiazolinethione fragment, which is slightly modified with the appearance of a shoulder at 270 nm, although the maximum is still located at 320 nm. As for **2**-Zn, the aggregation of **5**-Zn is illustrated by a blue-shifted quenched fluorescence (Figure S3 in the Supporting Information). The identical behaviour of **2**-Zn and **5**-Zn during aggregation makes the latter a good chiral model of the former. It should be noted that the optical purity of **5**-Zn has no impact on the global supramolecular organisation because the self-assemblies of (*rac*)-**5**-Zn, (*aR*)-**5**-Zn and (*aS*)-**5**-Zn produce the same results.

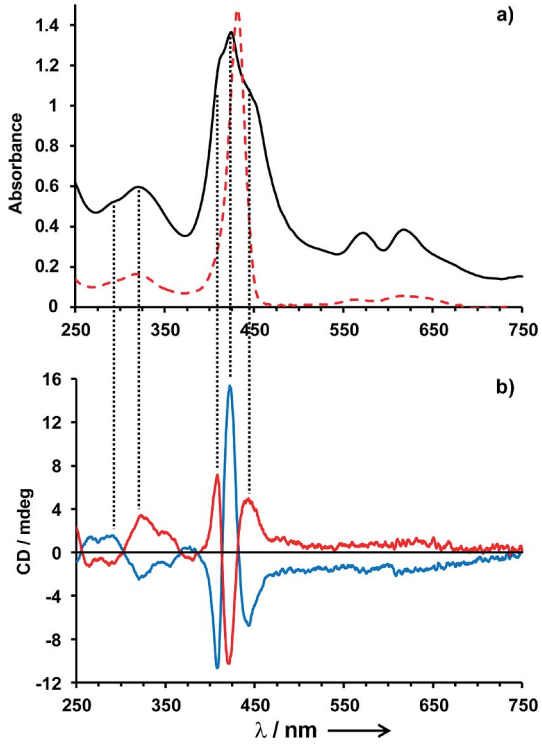

Figure 5. (a) UV/Vis spectra. Solid trace: dilution of a dry, concentrated dichloromethane solution of (*aR*)-**5**-Zn in *n*-heptane multiplied by 10. Dashed red trace: the same solution after addition of methanol. (b) ECD spectra. Red trace: dilution of a dry, concentrated dichloromethane solution of (*aS*)-**5**-Zn in *n*-heptane. Blue trace: dilution of a dry, concentrated dichloromethane solution of (*aR*)-**5**-Zn in *n*-heptane.

Monitoring of the aggregation of (*aR*)-**5**-Zn or (*aS*)-**5**-Zn by ECD spectroscopy revealed intense trisignate Cotton effects in the Soret band domain (Figure 5, b). This strong signature can only be attributed to the chiral packing of optically pure **5**-Zn because it disappears when the ECD spectra of (*aR*)-**5**-Zn and (*aS*)-**5**-Zn monomers are recorded (Figure S4 in the Supporting Information). When the corresponding free bases (*rac*)-**5**-2H, (*aR*)-**5**-2H and (*aS*)-**5**-2H were subjected to the same assembling procedure, the resulting UV/Vis spectra were only strongly broadened due to the precipitation of the monomers; the ECD spectra did not reveal any chiral signature in the Soret band domain (Figure S5 in the Supporting Information). These results confirm that the metal ligation process is crucial for supramolecular organisation of **5**-Zn and that the induction source of the observed supramolecular chirality is brought about by the chiral thiazolinethione fragment. If the chiral element is not directly linked to the metal centre, the helicity of **5**-Zn aggregates is probably driven by a steric repulsion between the thiazoline fragment of one monomer and the *meso*-phenyl substituent of the linked monomer producing a chiral J-dimer (Scheme 5). Another explanation would be the participation of the chiral thiazoline fragments, which have a strong dipolar moment of ca. 7 D[13] in secondary supramolecular interactions such as π-π interactions and H-bonding through the NH moieties of the urea, which would stabilise the overall packing of the chromophores. Theoretical calculations could shed light on these interactions and explain the translation of chirality from the molecular to the supramolecular level.

The ECD spectrum of (*aS*)-**5**-Zn aggregates displays a positive band at 443 nm, a strong negative band at 424 nm and a third positive band at 408 nm, whereas the (*aR*)-**5**-Zn assembly gives, as expected, the mirror-image induced ECD spectrum. The ECD signals of the thiazolinethione are affected by the packing of optically pure **5**-Zn, which transforms the same sign signals of the monomer into an alternate positive–negative bisignate ECD band that probably results from excitonic couplings between thiazolinethione fragments. The trisignate profile of the ECD spectra of **5**-Zn aggregates coincides exactly with the Soret maxima observed in the UV/Vis spectrum, which are fully assigned thanks to the alternating signs of the ECD bands. We chose to use the so-called "circular oscillator model" approach to describe the shapes of the ECD spectra. In this model, both Soret components (B_x and B_y) are equally weighted to predict Soret exciton chirality.[14] The interaction of two **5**-Zn monomers through Zn–NH intermolecular interactions produces two effective transition dipoles B_XB_X and B_YB_Y (Scheme 4). When two H-dimers are assembled in a chiral oblique J-tetramer, the transition dipoles B_XB_X and B_YB_Y interact and afford four permitted UV/Vis transitions A, B, Y and Z. According to the exciton chirality method, the ECD spectrum would then display two consecutive couplets of opposite chirality.[15] The negative twist between the interacting effective transition dipoles will produce a negative exciton couplet in the low energy domain whereas a positive couplet will be observed in the high-energy spectral region. The trisignate observed in the ECD spectra during the self-assembly of optically pure (*aR*)-**5**-Zn confirms this hypothesis and results from the mutual addition of the iso-energetic transitions B and Y that correspond to clockwise inter-dimer couplings of dipoles B_XB_X and B_YB_Y (Scheme 4). The equal energies of transitions B and Y are illustrated by the intensity of the central maximum, which is roughly the sum of the intensities of the two other maxima of opposite sign.

Conclusions

The noncatalysed nucleophilic aromatic substitution is a powerful tool that can be used to introduce functional groups on the porphyrin moiety.[5,16] We have used this procedure to prepare (bacterio)chlorophyll mimics in which the two recognition groups of the zinc porphyrin are placed on the same side of the porphyrin macrocycle. The stable and favoured 5½ coordination of the zinc ion produces a novel packing of the chromophores. The stronger metal–ligand interaction produces H- or J-dimers that are assembled, thanks to the weaker metal–ligand bond, into J- or H-type higher oligomers. A similar model was used to describe the solid H-packing of chiral bisporphyrins leading to tetramers with complex ECD spectra.[11b] The aggregation of the dimers is due to weak secondary interactions that are very labile and less probable. Therefore, the largest component of the species in solution seems to be tetramers, which can be formed with only a single weak interdimer interaction. The chirality of chromophore aggregates can be induced by, or transferred through, strong intermolecular interactions such as a chiral metal–ligation, hydrogen bonds or electrostatic interactions.[17] We report here how an optically pure atropisomer induces, through weak secondary supramolecular interactions, a helicity and is used as a chiral probe to reveal the complex spectroscopic features of a novel supramolecular organisation. This spatial arrangement causes a concomitant blueshift and redshift of the UV/Vis absorption, which is crucial for constructing efficient light-harvesting systems. We are now working on the preparation of derivatives bearing two identical recognition groups to produce larger assemblies that should display both J- and H-type architectures.

Experimental Section

General Remarks: All reagents were used as received. Tetrahydrofuran (THF) was distilled from sodium and benzophenone. Dichloromethane (CH_2Cl_2), *n*-hexane and *n*-heptane were distilled over calcium hydride. Flash column chromatography was performed on silica gel 60 (230–400 mesh).

^{1}H NMR spectra were recorded with a Bruker Avance 300, a Bruker Avance 200 or a Bruker Avance 400 Ultrashield NMR spectrometer. Chemical shifts are given in ppm relative to residual peaks of chloroform (δ = 7.26 ppm) or dimethyl sulfoxide (δ = 2.50 ppm). Diffusion experiments were recorded with a Bruker Avance 400 Ultrashield NMR spectrometer. The sequence corresponds to Bruker pulse program *ledbpgp2s* using stimulated echo, bipolar gradients and longitudinal eddy current delay as *z* filter. The four 2 ms gradients pulses have sine-bell shapes and ampli-

tudes ranging linearly from 2 to 33 G m^{-1} cm^{-1} in 16 steps. The diffusion delay was 250 ms and the number of scans 32 (P_1 = 9 µs, PL_1 = 0 db). The processing was done using a line broadening of 1 Hz and the diffusion rates *Dx* calculated using the Bruker processing package, by analysing the decay of the natural logarithm of the normalised signal intensity I/I_0 of selected NMR signals as a function of the square of the pulse gradient strength according to Equation (1) [*I* is the observed intensity, I_0 is the intensity without gradients, γ is the gyromagnetic ratio of the observed nucleus, δ is the length of the gradient pulse, *G* is the gradient strength, D (diffusion delay) is the delay between the midpoints of the gradients].

$$\ln(I/I_0) = -(\gamma\delta)^2(\Delta - \delta/3)DG^2 \quad (1)$$

The NMR tubes were prepared by dissolving the selected compound (17 µmol, ca. 10 mg) in DMSO (0.6 mL). The sample temperature was controlled and stabilised at 30 °C.

UV/Vis spectra were measured with a Shimadzu UV-2401 (PC) instrument. Fluorescence emission spectra were recorded with a Varian Cary Eclipse spectrofluorimeter. ECD spectra were measured with a JASCO J-815 spectrometer equipped with a JASCO Peltier cell holder PTC-423 to maintain the temperature at 20.0 ± 0.2 °C. Hellma quartz cells of 1 cm optical pathlength were used. Solutions were prepared by dilution of solid samples in CH_2Cl_2 (HPLC grade). The ECD spectrometer was purged with nitrogen before recording each spectrum, which was baseline subtracted. The baseline was always measured for the same solvent and in the same cell as the samples. The spectra are presented without smoothing or further data processing. High-resolution mass spectrometry (HRMS-ESI) analyses were performed with a QStar Elite (Applied Biosystems SCIEX) spectrometer or with a SYNAPT G2 HDMS (Waters) spectrometer. These two instruments were equipped with an electrospray ionisation source and were used in the positive ion mode and with a capillary voltage set at +5500 V. The preliminary screening of chiral stationary phases was performed with a Lachrom-Elite unit consisting of an L-2130 pump, an L-2200 autosampler, an L-2350 oven and an L-2455 DAD detector. The analytical columns (250 × 4.6 mm) tested were Chiralpak IA, IB and IC columns from Chiral Technology Europa (Illkirch, France), Whelk-O1 (*S*,*S*) and Ulmo (*S*,*S*) from Regis Technologies (Morton Grove, USA). *n*-Hexane and ethanol, HPLC grade, were degassed and filtered through a 0.45 µm millipore membrane before use. Retention times (R_t) in minutes, retention factors $k_i = (Rt_i - Rt_0)/Rt_0$ and enantioselectivity factor $\alpha = k_2/k_1$ are given. Rt_0 was determined by injection of tri-*tert*-butylbenzene.

CCDC-876244 (for **3**-2H) contains the supplementary crystallographic data for this paper. These data can be obtained free of charge from The Cambridge Crystallographic Data Centre via www.ccdc.cam.ac.uk/data_request/cif.

The *N*-(2-aminophenyl)-4-methylthiazoline-2-thiones (*rac*)-**7**, (*aR*)-**7**, (*aS*)-**7** and thiazolinethione **13** were prepared and purified according to literature procedures.[6,7]

(5,15-Diphenylporphyrinato)zinc (9-Zn): Prepared by metalation of 5,15-diphenylporphyrin[18] according to a literature procedure.[19] R_f = 0.68 (MeOH/CH_2Cl_2, 0.5:99.5). ^{1}H NMR (200 MHz, $CDCl_3$, 25 °C): δ = 10.21 (s, 2 H, H-*meso*), 9.35 [d, $^3J_{H,H}$ = 4.5 Hz, 4 H, H-β], 9.05 [d, $^3J_{H,H}$ = 4.5 Hz, 4 H, H-β], 8.21–8.25 (m, 4 H, Ar-H), 7.73–7.76 (m, 4 H, Ar-H) ppm. UV/Vis ($CHCl_3$): λ_{max} ($\log\varepsilon_{max}$) = 413 (5.62), 541 nm (4.22).

5-Bromo-10,15,20-triphenylporphyrin (6): This compound was prepared according to a literature procedure.[20] 5,10,15-Triphenylporphyrine[21] (753 mg, 1.4 mmol, 1 equiv.) and pyridine (450 µL, 5.6 mmol, 4 equiv.) were dissolved in $CHCl_3$ (300 mL) under argon at 0 °C. *N*-Bromosuccinimide (348 mg, 1.96 mmol, 1.4 equiv.) was added and the disappearance of the starting porphyrin was monitored by TLC. After 20 min, acetone (15 mL) was added and the mixture was washed with water (3 × 300 mL), dried with Na_2SO_4 and the solvents evaporated. After recrystallisation from CH_2Cl_2/*n*-heptane, porphyrin **6** (856 mg, 1.38 mmol, 99%) was obtained as a dark-violet solid. R_f = 0.41 (CH_2Cl_2/*n*-hexane, 2:3). ^{1}H NMR (200 MHz, $CDCl_3$, 25 °C): δ = 9.66 [d, $^3J_{H,H}$ = 5.1 Hz, 2 H, H-β], 8.89 [d, $^3J_{H,H}$ = 5.1 Hz, 2 H, H-β], 8.80 (s, 4 H, H-β), 8.15–8.21 (m, 6 H, Ar-H), 7.72–7.79 (m, 9 H, Ar-H), –2.75 (s, 2 H, NH) ppm. UV/Vis ($CHCl_3$): λ_{max} ($\log\varepsilon_{max}$) = 420 (5.59), 518 (4.26), 553 (3.97), 595 (3.73), 651 nm (3.64).

5-Propylamino-10,15,20-triphenylporphyrin (3-2H): 5-Bromo-10,15,20-triphenylporphyrin (**6**) (180 mg, 291 µmol) and propylamine (4.8 mL, 58 mmol, 200 equiv.) were dissolved in THF (3 mL). The mixture was heated to reflux for 20 h. After evaporation, the resulting solid was purified by chromatography on silica gel (CH_2Cl_2/*n*-hexane, 7:3). After evaporation, porphyrin **3**-2H (154 mg, 259 µmol, 89%) was obtained as a dark-violet solid. R_f = 0.27 (CH_2Cl_2/*n*-hexane, 7:3). ^{1}H NMR (200 MHz, $CDCl_3$, 25 °C): δ = 9.16 [d, $^3J_{H,H}$ = 4.7 Hz, 2 H, H-β], 8.62 [d, $^3J_{H,H}$ = 4.8 Hz, 2 H, H-β], 8.58 [d, $^3J_{H,H}$ = 4.5 Hz, 2 H, H-β], 8.57 [d, $^3J_{H,H}$ = 4.7 Hz, 2 H, H-β], 8.15–8.17 (m, 4 H, Ar-H), 8.12–8.13 (m, 2 H, Ar-H), 7.70–7.76 (m, 9 H, Ar-H), 6.12 (s, 1 H, N*H*CH_2), 4.36 [t, $^3J_{H,H}$ = 6.2 Hz, 2 H, CH_2NH], 2.06 [sext, $^3J_{H,H}$ = 7.3 Hz, 2 H, CH_2CH_3], 1.18 [t, $^3J_{H,H}$ = 7.4 Hz, 3 H, CH_3], –1.40 (s, 2 H, NH_{pyr}) ppm. UV/Vis ($CHCl_3$): λ_{max} ($\log\varepsilon_{max}$) = 427 (5.52), 531 (3.89), 583 (4.17), 681 nm (4.01). HRMS (ESI): calcd. for $C_{41}H_{34}N_5^+$ 596.2809 [M + H]$^+$; found 596.2810. Single crystals of porphyrin **3**-2H were grown by slow diffusion of *n*-heptane into a concentrated solution of porphyrin **3**-2H in dichloromethane.

5-(2-Aminoethylamino)-10,15,20-triphenylporphyrin (4-2H): 5-Bromo-10,15,20-triphenylporphyrin (**6**) (315 mg, 0.51 mmol) and ethylenediamine (6.8 mL, 102 mmol, 200 equiv.) were dissolved in THF (6 mL). The mixture was heated to reflux for 24 h. After evaporation, the crude residue was dissolved in CH_2Cl_2 (80 mL), washed with distilled water (5 × 100 mL) and dried with $MgSO_4$. The resulting solid was purified by chromatography on silica gel (CH_2Cl_2/MeOH/Et_3N, 98.5:0.5:1). After evaporation, porphyrin **4**-2H (260 mg, 0.433 mmol, 85%) was obtained as a dark-violet solid. R_f = 0.24 (CH_2Cl_2/MeOH, 9:1). ^{1}H NMR (200 MHz, $CDCl_3$, 25 °C): δ = 9.27 [d, $^3J_{H,H}$ = 4.6 Hz, 2 H, H-β], 8.62 [d, $^3J_{H,H}$ = 4.8 Hz, 2 H, H-β], 8.58 [d, $^3J_{H,H}$ = 4.8 Hz, 2 H, H-β], 8.56 [d, $^3J_{H,H}$ = 4.8 Hz, 2 H, H-β], 8.10–8.19 (m, 6 H, Ar-H), 7.70–7.75 (m, 9 H, Ar-H), 4.38 [t, $^3J_{H,H}$ = 5.6 Hz, 2 H, CH_2NH], 3.23 [t, $^3J_{H,H}$ = 5.6 Hz, 2 H, CH_2NH_2], –1.42 (s, 2 H, $NH_{pyrrole}$) ppm. UV/Vis ($CHCl_3$): λ_{max} ($\log\varepsilon_{max}$) = 426 (5.48), 531 (3.89), 581 (4.13), 679 nm (3.97). HRMS (ESI): calcd. for $C_{40}H_{33}N_6^+$ 597.2761 [M + H]$^+$; found 597.2774.

(5-Propylamino-10,15,20-triphenylporphyrinato)zinc (3-Zn): 5-Propylamino-10,15,20-triphenylporphyrin (**3**-2H) (100 mg, 168 µmol, 1 equiv.) and zinc acetate dihydrate (55 mg, 252 µmol, 1.5 equiv.) were dissolved in a mixture of CH_2Cl_2/MeOH (12 mL, 4:1). The mixture was stirred at room temperature for 3 h. The mixture was washed successively with saturated aqueous $NaHCO_3$ (30 mL), water (2 × 30 mL) and dried with $MgSO_4$. After evaporation, the resulting solid was purified by chromatography on silica gel (CH_2Cl_2/MeOH, 99.5:0.5). After recrystallisation from CH_2Cl_2/*n*-heptane, **3**-Zn (110 mg, 166 µmol, 99%) was obtained as a dark-violet solid. R_f = 0.63 (CH_2Cl_2/MeOH, 99.5:0.5). ^{1}H NMR (400 MHz, [D_6]DMSO, 25 °C): δ = 9.40 [d, $^3J_{H,H}$ = 4.8 Hz, 2 H, H-β], 8.45 [d, $^3J_{H,H}$ = 4.4 Hz, 2 H, H-β], 8.38 [d, $^3J_{H,H}$ = 4.4 Hz,

4 H, H-β], 8.06–8.09 (m, 4 H, Ar-H), 8.02–8.04 (m, 2 H, Ar-H), 7.74–7.76 (m, 6 H, Ar-H), 7.70–7.72 (m, 3 H, Ar-H), 7.58 [t, $^3J_{H,H}$ = 7.2 Hz, 1 H, N*H*CH_2], 4.30 [q, $^3J_{H,H}$ = 7.2 Hz, 2 H, CH_2NH], 2.01 [sext, $^3J_{H,H}$ = 7.2 Hz, 2 H, C$H_2$$CH_3$], 1.02 [t, $^3J_{H,H}$ = 7.2 Hz, 3 H, CH_3] ppm. UV/Vis ($CHCl_3$): λ_{max} ($\log\varepsilon_{max}$) = 431 (5.54), 564 (4.00), 611 nm (4.09). HRMS (ESI): calcd. for $C_{41}H_{32}N_5Zn^+$ 658.1944 [M + H]$^+$; found 658.1951.

[5-(2-Aminoethylamino)-10,15,20-triphenylporphyrinato]zinc (4-Zn): 5-(2-Aminoethylamino)-10,15,20-triphenylporphyrin (**4**-2H) (80 mg, 134 μmol, 1 equiv.) and zinc acetate dihydrate (44 mg, 201 μmol, 1.5 equiv.) were dissolved in a mixture of CH_2Cl_2/MeOH (25 mL, 4:1). The mixture was stirred at room temperature for 3 h. The mixture was washed successively with saturated aqueous $NaHCO_3$ (40 mL), water (2 × 40 mL) and dried with $MgSO_4$. After evaporation, the resulting solid was purified by chromatography on silica gel (CH_2Cl_2/MeOH/Et_3N, 98.5:0.5:1, then CH_2Cl_2/MeOH, 99.5:0.5). After recrystallisation from CH_2Cl_2/*n*-heptane, zinc porphyrin **4**-Zn (75 mg, 114 μmol, 85%) was obtained as a dark-violet solid. R_f = 0.12 (CH_2Cl_2/MeOH, 99.5:0.5). ^{1}H NMR (400 MHz, [D$_6$]DMSO, 25 °C): δ = 8.62 [d, $^3J_{H,H}$ = 4.1 Hz, 2 H, H-β], 8.54 [d, $^3J_{H,H}$ = 4.6 Hz, 2 H, H-β], 8.48 [d, $^3J_{H,H}$ = 4.6 Hz, 2 H, H-β], 8.23 [d, $^3J_{H,H}$ = 4.4 Hz, 2 H, H-β], 8.15–8.17 (m, 4 H, Ar-H), 8.10–8.12 (m, 2 H, Ar-H), 7.77–7.78 (m, 6 H, Ar-H), 7.74–7.75 (m, 3 H, Ar-H), 6.38 (s, 1 H, N*H*CH_2), 2.91 (s, 2 H, CH_2NH), –0.59 (s, 2 H, C$H_2$$NH_2$), –1.32 (s, 2 H, NH_2) ppm. UV/Vis ($CHCl_3$): λ_{max} ($\log\varepsilon_{max}$) = 432 (5.45), 575 (3.98), 622 nm (4.16). HRMS (ESI): calcd. for $C_{40}H_{31}N_6Zn^+$ 659.1896 [A + H]$^+$; found 659.1902; calcd. for $C_{80}H_{60}N_{12}Zn_2Na^+$ 1343.3521 (Isotopic maximum) [2A + Na]$^+$; found 1343.3518 (isotopic maximum).

5-(2-{2-[4-Methyl-2-thioxothiazol-3(2*H*)-yl]phenylureido}ethylamino)-10,15,20-triphenylporphyrin [(*rac*)-5-2H]: Triphosgene (61 mg, 208 μmol, 0.53 equiv.) was dissolved in freshly distilled CH_2Cl_2 (7 mL) under argon at 0 °C before a solution of (*rac*)-*N*-(2-aminophenyl)-4-methylthiazoline-2-thione (*rac*)-**7** (138 mg, 623 μmol, 1.6 equiv.) and diisopropylethylamine (222 μL, 1247 μmol, 3.2 equiv.) in freshly distilled CH_2Cl_2 (8 mL) was added. The mixture was stirred at room temperature for 90 min, and the formation of isocyanate (*rac*)-**8** was monitored by TLC [R_f = 0.80 (CH_2Cl_2/AcOEt, 4:1)]. A solution of 5-(2-aminoethylamino)-10,15,20-triphenylporphyrin (**4**-2H) (233 mg, 391 μmol, 1 equiv.) in freshly distilled CH_2Cl_2 (9 mL) was added and the mixture was stirred at room temperature for 30 min. The mixture was washed successively with saturated aqueous $NaHCO_3$ (20 mL), water (20 mL) and dried with $MgSO_4$. After evaporation, the resulting solid was purified by chromatography on silica gel (CH_2Cl_2/AcOEt/Et_3N, 80:19:1). After recrystallisation from CH_2Cl_2/*n*-heptane, porphyrin (*rac*)-**5**-2H (287 mg, 340 μmol, 87%) was obtained as a dark-violet solid. R_f = 0.14 (CH_2Cl_2/AcOEt/Et_3N, 80:19:1). ^{1}H NMR (400 MHz, $CDCl_3$, 25 °C): δ = 9.00 [d, $^3J_{H,H}$ = 4.4 Hz, 2 H, H-β], 8.52 [d, $^3J_{H,H}$ = 4.8 Hz, 2 H, H-β], 8.45 [d, $^3J_{H,H}$ = 4.8 Hz, 2 H, H-β], 8.38 [d, $^3J_{H,H}$ = 4.4 Hz, 2 H, H-β], 8.07–8.08 (m, 6 H, Ar-H), 7.92 [d, $^3J_{H,H}$ = 8.0 Hz, 1 H, Ar-H], 7.67–7.71 (m, 10 H, Ar-H, Ar-N*H*), 7.36 [t, $^3J_{H,H}$ = 7.6 Hz, 1 H, Ar-H], 7.11 [t, $^3J_{H,H}$ = 7.6 Hz, 1 H, Ar-H], 6.88 (br. s, 1 H, CH_2N*H*-CO), 6.80 [d, $^3J_{H,H}$ = 7.6 Hz, 1 H, Ar-H], 5.95 [t, $^3J_{H,H}$ = 5.8 Hz, 1 H, CH_2N*H*], 5.09 (s, 1 H, S-C*H*), 4.25 (m, 2 H, CH_2-NHCO), 3.57 (m, 2 H, CH_2-NH), 1.24 (s, 3 H, CH_3), –1.08 (s, 2 H, $NH_{pyrrole}$) ppm. UV/Vis ($CHCl_3$): λ_{max} ($\log\varepsilon_{max}$) = 324 (4.32), 426 (5.51), 522 (3.69), 587 (4.02), 682 nm (3.91). HRMS (ESI): calcd. for $C_{51}H_{41}N_8OS_2^+$ 845.2839 [M + H]$^+$; found 845.2844. Chiral HPLC (Chiralpak IC; *n*-hexane/ethanol, 4:1; 1 mL/min; UV 420 nm) Rt_1 (*aR*) = 16.97 min, Rt_2 (*aS*) = 21.93 min, k_1 (*aR*) = 4.66, k_2 (*aS*) = 6.31, α = 1.35, Rs = 2.71.

(*aS*)-5-(2-{2-[4-Methyl-2-thioxothiazol-3(2*H*)-yl]phenylureido}ethylamino)-10,15,20-triphenylporphyrin [(*aS*)-5-2H]: Prepared as for porphyrin (*rac*)-**5**-2H starting from triphosgene (31 mg, 107 μmol, 0.53 equiv.), pure (*aS*)-*N*-(2-aminophenyl)-4-methylthiazoline-2-thione (*aS*)-**7** (71 mg, 320 μmol, 1.6 equiv.), diisopropylethylamine (114 μL, 641 μmol, 3.2 equiv.) and porphyrin **4**-2H (120 mg, 201 μmol, 1 equiv.). Porphyrin (*aS*)-**5**-2H (143 mg, 169 μmol, 84%) was obtained as a dark-violet solid. Chiral HPLC (Chiralpak IC; *n*-hexane/ethanol, 4:1; 1 mL/min; UV 420 nm): R_t = 21.95 min.

(*aR*)-5-(2-{2-[4-Methyl-2-thioxothiazol-3-(2*H*)-yl]phenylureido}ethylamino)-10,15,20-triphenylporphyrin [(*aR*)-5-2H]: Prepared as for the porphyrin (*rac*)-**5**-2H starting from triphosgene (31 mg, 107 μmol, 0.53 equiv.), pure (*aR*)-*N*-(2-aminophenyl)-4-methylthiazoline-2-thione (*aR*)-**7** (71 mg, 320 μmol, 1.6 equiv.), diisopropylethylamine (114 μL, 641 μmol, 3.2 equiv.) and porphyrin **4**-2H (120 mg, 201 μmol, 1 equiv.). Porphyrin (*aR*)-**5**-2H (134 mg, 159 μmol, 79%) was obtained as a dark-violet solid. Chiral HPLC (Chiralpak IC; *n*-hexane/ethanol, 4:1; 1 mL/min; UV 420 nm): R_t = 16.83 min.

5-[2-(Phenylureido)ethylamino]-10,15,20-triphenylporphyrin (2-2H): 5-(2-Aminoethylamino)-10,15,20-triphenylporphyrin (**4**-2H) (100 mg, 0.168 mmol) and phenyl isocyanate (24 μL, 0.218 mmol, 1.3 equiv.) were dissolved in freshly distilled CH_2Cl_2 (10 mL). The mixture was stirred at room temperature for 30 min. After evaporation, the resulting solid was purified by chromatography on silica gel (CH_2Cl_2/AcOEt/Et_3N, 80:19:1). After recrystallisation from CH_2Cl_2/*n*-heptane, porphyrin **2**-2H (104 mg, 0.145 mmol, 86%) was obtained as a dark-violet solid. R_f = 0.09 (CH_2Cl_2/AcOEt/Et_3N, 80:19:1). ^{1}H NMR (400 MHz, [D$_6$]DMSO, 25 °C): δ = 9.36 [d, $^3J_{H,H}$ = 4.7 Hz, 2 H, H-β], 8.61 (s, 1 H, Ar-N*H*-CO), 8.59 [t, $^3J_{H,H}$ = 5.4 Hz, 1 H, CH_2N*H*-CO], 8.36 [d, $^3J_{H,H}$ = 4.9 Hz, 2 H, H-β], 8.28 [d, $^3J_{H,H}$ = 4.9 Hz, 2 H, H-β], 8.23 [d, $^3J_{H,H}$ = 4.7 Hz, 2 H, H-β], 8.04–8.06 (m, 4 H, Ar-H), 8.00–8.03 (m, 2 H, Ar-H), 7.75–7.78 (m, 6 H, Ar-H), 7.71–7.74 (m, 3 H, Ar-H), 7.35 [t, $^3J_{H,H}$ = 7.6 Hz, 2 H, Ar-H], 7.18 [t, $^3J_{H,H}$ = 7.9 Hz, 2 H, Ar-H], 6.88 [d, $^3J_{H,H}$ = 7.3 Hz, 1 H, Ar-H], 6.59 [t, $^3J_{H,H}$ = 5.8 Hz, 1 H, CH_2N*H*], 4.25 [q, $^3J_{H,H}$ = 5.7 Hz, 2 H, CH_2-NHCO], 3.57 [q, $^3J_{H,H}$ = 5.8 Hz, 2 H, CH_2-NH], –0.38 (s, 2 H, $NH_{pyrrole}$) ppm. UV/Vis ($CHCl_3$): λ_{max} ($\log\varepsilon_{max}$) = 428 (5.56), 587 (4.22), 682 nm (4.17). HRMS (ESI): calcd. for $C_{47}H_{38}N_7O^+$ 716.3132 [M + H]$^+$; found 716.3139.

{5-[2-(Phenylureido)ethylamino]-10,15,20-triphenylporphyrinato}zinc (2-Zn): 5-[2-(Phenylureido)ethylamino]-10,15,20-triphenylporphyrin (**2**-2H) (90 mg, 126 μmol, 1 equiv.) and zinc acetate dihydrate (30 mg, 138 μmol, 1.1 equiv.) were dissolved in a mixture of CH_2Cl_2/MeOH (30 mL, 4:1). The mixture was stirred at room temperature for 3 h then washed successively with saturated aqueous $NaHCO_3$ (50 mL), water (2 × 30 mL) and dried with $MgSO_4$. After evaporation, the resulting solid was purified by chromatography on silica gel (CH_2Cl_2/MeOH, 98:2). After recrystallisation from CH_2Cl_2/*n*-heptane, zinc porphyrin **2**-Zn (75 mg, 97 μmol, 77%) was obtained as a dark-green solid. R_f = 0.34 (CH_2Cl_2/MeOH, 9:1). ^{1}H NMR (400 MHz, [D$_6$]DMSO, 25 °C): δ = 9.46 [d, $^3J_{H,H}$ = 4.6 Hz, 2 H, H-β], 8.63 (s, 1 H, Ar-N*H*-CO), 8.45 [d, $^3J_{H,H}$ = 4.6 Hz, 2 H, H-β], 8.39 [d, $^3J_{H,H}$ = 4.6 Hz, 2 H, H-β], 8.38 [d, $^3J_{H,H}$ = 4.5 Hz, 2 H, H-β], 8.05–8.08 (m, 4 H, Ar-H), 8.02–8.04 (m, 2 H, Ar-H), 7.73–7.77 (m, 7 H, Ar-H, CH_2-N*H*-CO), 7.70–7.72 (m, 3 H, Ar-H), 7.38 [d, $^3J_{H,H}$ = 7.6 Hz, 2 H, Ar-H], 7.20 [t, $^3J_{H,H}$ = 7.8 Hz, 2 H, Ar-H], 6.88 [t, $^3J_{H,H}$ = 7.4 Hz, 2 H, Ar-H], 6.61 [t, $^3J_{H,H}$ = 5.8 Hz, 1 H, CH_2N*H*], 4.40 [q, $^3J_{H,H}$ = 6.0 Hz, 2 H, CH_2-NHCO], 3.77 [q, $^3J_{H,H}$ = 6.0 Hz, 2 H, CH_2-NH] ppm. UV/Vis ($CHCl_3$): λ_{max} ($\log\varepsilon_{max}$) = 431 (5.41), 565 (3.97), 613 nm (4.05). HRMS (ESI): calcd. for $C_{47}H_{36}N_7OZn^+$ 778.2267 [M + H]$^+$; found 778.2249.

[5-(2-{2-[4-Methyl-2-thioxothiazol-3(2*H*)-yl]phenylureido}-ethylamino)-10,15,20-triphenylporphyrinato]zinc [(*rac*)-5-Zn]: The free-base porphyrin (*rac*)-**5**-2H (200 mg, 237 μmol, 1 equiv.) and zinc acetate dihydrate (52 mg, 237 μmol, 1 equiv.) were dissolved in a mixture of CH_2Cl_2/MeOH (60 mL, 4:1). The mixture was stirred at room temperature for 3 h then washed successively with saturated aqueous $NaHCO_3$ (80 mL), water (2 × 80 mL) and dried with $MgSO_4$. After evaporation, the resulting solid was purified by chromatography on silica gel (CH_2Cl_2/MeOH, 98:2). After recrystallisation from CH_2Cl_2/*n*-heptane, the zinc porphyrin (*rac*)-**5**-Zn (177 mg, 195 μmol, 82%) was obtained as a dark-green solid. R_f = 0.13 (CH_2Cl_2/MeOH, 98:2). ^{1}H NMR (400 MHz, [D$_6$]DMSO, 25 °C): δ = 9.46 [d, $^3J_{H,H}$ = 4.8 Hz, 2 H, H-β], 8.48 [d, $^3J_{H,H}$ = 4.8 Hz, 2 H, H-β], 8.42 [d, $^3J_{H,H}$ = 4.8 Hz, 2 H, H-β], 8.41 [d, $^3J_{H,H}$ = 4.8 Hz, 2 H, H-β], 8.18 [d, $^3J_{H,H}$ = 8.4 Hz, 1 H, Ar-H], 8.07–8.09 (m, 4 H, Ar-H), 8.04–8.06 (m, 2 H, Ar-H), 7.75–7.77 (m, 6 H, Ar-H), 7.71–7.73 (m, 3 H, Ar-H), 7.64 (s, 2 H, N*H*-CO), 7.41 (ddd, $^3J_{H,H}$ = 8.8, $^3J_{H,H}$ = 6.8, $^4J_{H,H}$ = 2.0 Hz, 1 H, Ar-H), 7.35 (t, $^3J_{H,H}$ = 5.8 Hz, 1 H, CH_2N*H*), 7.08–7.14 (m, 2 H, Ar-H), 6.73 (d, $^3J_{H,H}$ = 1 Hz, 1 H, S-C*H*), 4.37 (br. s, 2 H, C*H*$_2$-NHCO), 3.74 (q, $^3J_{H,H}$ = 6.0 Hz, 2 H, C*H*$_2$-NH), 1.24 (d, $^4J_{H,H}$ = 1 Hz, 3 H, CH_3) ppm. UV/Vis ($CHCl_3$): λ_{max} (log ε_{max}) = 319 (4.47), 430 (5.49), 561 (4.03), 613 nm (4.02). HRMS (ESI): calcd. for $C_{51}H_{39}N_8OS_2Zn^+$ 907.1974 [M + H]$^+$; found 907.1961.

[(*aS*)-5-(2-{2-[4-Methyl-2-thioxothiazol-3(2*H*)-yl]phenylureido}-ethylamino)-10,15,20-triphenylporphyrinato]zinc [(*aS*)-5-Zn]: Prepared as for porphyrin (*rac*)-**5**-Zn starting from porphyrin (*aS*)-**5**-2H (75 mg, 88 μmol, 1 equiv.) and zinc acetate dihydrate (19 mg, 88 μmol, 1 equiv.). Zinc porphyrin (*aS*)-**5**-Zn (73 mg, 80 μmol, 91%) was obtained as a dark-green solid.

[(*aR*)-5-(2-{2-[4-Methyl-2-thioxothiazol-3(2*H*)-yl]phenylureido}-ethylamino)-10,15,20-triphenylporphyrinato]zinc [(*aR*)-5-Zn]: Prepared as for porphyrin (*rac*)-**5**-Zn starting from porphyrin (*aR*)-**5**-2H (75 mg, 88 μmol, 1 equiv.) and zinc acetate dihydrate (19 mg, 88 μmol, 1 equiv.). Zinc porphyrin (*aR*)-**5**-Zn (73 mg, 80 μmol, 91%) was obtained as a dark-green solid.

Supporting Information (see footnote on the first page of this article): Structural analysis of porphyrin **3**-2H, supplementary figures, DOSY NMR characterization of **4**-Zn J-dimer. ^{1}H NMR spectra of porphyrins **2**-Zn, **3**-Zn and **5**-Zn.

Acknowledgments

The autors thank Melanie Decostanzi for her assistance in the synthesis of precursors.

[1] T. S. Balaban, in: *Handbook of Porphyrin Science with Applications to Chemistry, Physics, Materials Science Engineering, Biology and Medicine*, vol. 1 (Eds.: K. M. Kadish, K. M. Smith, R. Guilard), World Scientific, Singapore, **2010**, pp. 221–306.
[2] A. Satake, Y. Kobuke, *Org. Biomol. Chem.* **2007**, *5*, 1679–1691.
[3] a) T. S. Balaban, *Acc. Chem. Res.* **2005**, *38*, 612–623; b) T. S. Balaban, A. D. Bhise, M. Fischer, M. Linke-Schaetzel, C. Roussel, N. Vanthuyne, *Angew. Chem.* **2003**, *115*, 2190–2194; *Angew. Chem. Int. Ed.* **2003**, *42*, 2140–2144.
[4] T. Jochum, C. M. Reddy, A. Eichhöfer, G. Buth, J. Szmytkowski, H. Kalt, D. Moss, T. S. Balaban, *Proc. Natl. Acad. Sci. USA* **2008**, *105*, 12736–12741.
[5] M. C. Balaban, C. Chappaz-Gillot, G. Canard, O. Führ, C. Roussel, T. S. Balaban, *Tetrahedron* **2009**, *65*, 3733–3739.
[6] N. Vanthuyne, F. Andreoli, S. Fernandez, M. Roman, C. Roussel, *Lett. Org. Chem.* **2005**, *2*, 433–443.
[7] a) C. Roussel, C. Popescu, *Chirality* **1994**, *6*, 251–260; b) C. Roussel, M. Roman, F. Andreoli, A. Del Rio, R. Faure, N. Vanthuyne, *Chirality* **2006**, *18*, 762–771.
[8] M. Kasha, H. R. Rawls, M. A. El-Bayoumi, *Pure Appl. Chem.* **1965**, *11*, 371–392.
[9] M. Gardner, A. J. Guerin, C. A. Hunter, U. Michelsen, C. Rotger, *New J. Chem.* **1999**, *23*, 309–316.
[10] a) F. Hajjaj, Z. S. Yoon, M.-C. Yoon, J. Park, A. Satake, D. Kim, Y. Kobuke, *J. Am. Chem. Soc.* **2006**, *128*, 4612–4623; b) R. Takahashi, Y. Kobuke, *J. Org. Chem.* **2005**, *70*, 2745–2753.
[11] a) X. Huang, K. Nakanishi, N. Berova, *Chirality* **2000**, *12*, 237–255; b) V. V. Borovkov, T. Harada, Y. Inoue, R. Kuroda, *Angew. Chem.* **2002**, *114*, 1436–1439; *Angew. Chem. Int. Ed.* **2002**, *41*, 1378–1381; c) V. V. Borovkov, T. Harada, G. A. Hembury, Y. Inoue, R. Kuroda, *Angew. Chem.* **2003**, *115*, 1788–1791; *Angew. Chem. Int. Ed.* **2003**, *42*, 1746–1749; d) N. Yoshida, T. Ishizuka, A. Osuka, D. H. Jeong, H. S. Cho, D. Kim, Y. Matsuzaki, A. Nogami, K. Tanaka, *Chem. Eur. J.* **2003**, *9*, 58–75; e) G. Bringmann, D. C. G. Götz, T. A. M. Gulder, T. H. Gehrke, T. Bruhn, T. Kupfer, K. Radacki, H. Braunschweig, A. Heckmann, C. Lambert, *J. Am. Chem. Soc.* **2008**, *130*, 17812–17825; f) A. Mammana, G. Pescitelli, T. Asakawa, S. Jockusch, A. G. Petrovic, R. R. Monaco, R. Purrello, N. J. Turro, K. Nakanishi, G. A. Ellestad, M. Balaz, N. Berova, *Chem. Eur. J.* **2009**, *15*, 11853–11866; g) I. Cohen-Ofri, M. van Gastel, J. Grzyb, A. Brandis, I. Pinkas, W. Lubitz, D. Noy, *J. Am. Chem. Soc.* **2011**, *133*, 9526–9535.
[12] a) H.-Y. Liu, J.-W. Huang, X. Tian, X.-D. Jiao, G.-T. Luo, L.-N. Ji, *Chem. Commun.* **1997**, 1575–1576; b) T. S. Balaban, M. Linke-Schaetzel, A. D. Bhise, N. Vanthuyne, C. Roussel, *Eur. J. Org. Chem.* **2004**, 3919–3930; c) Y. Matano, T. Shinokura, K. Matsumoto, H. Imahori, H. Nakano, *Chem. Asian J.* **2007**, *2*, 1417–1429; d) G. Gottarelli, S. Lena, S. Masiero, S. Pieraccini, G. P. Spada, *Chirality* **2008**, *20*, 471–485; e) L. Zeng, Y. He, Z. Dai, J. Wang, Q. Cao, Y. Zhang, *ChemPhysChem* **2009**, *10*, 954–962; f) P. Iavicoli, H. Xu, L. N. Feldborg, M. Linares, M. Paradinas, S. Stafström, C. Ocal, B. Nieto-Ortega, J. Casado, J. T. López Navarrete, R. Lazzaroni, S. D. Feyter, D. B. Amabilino, *J. Am. Chem. Soc.* **2010**, *132*, 9350–9362.
[13] *HyperChem*, v. 8.0, Hypercube, Inc., Gainsville, Florida.
[14] G. Pescitelli, S. Gabriel, Y. Wang, J. Fleischhauer, R. W. Woody, N. Berova, *J. Am. Chem. Soc.* **2003**, *125*, 7613–7628.
[15] a) N. Harada, K. Nakanishi, *Circular Dichroic Spectroscopy. Exciton Coupling in Organic Stereochemistry*, University Science Books, Mill Valley, CA, **1983**; b) N. Berova, K. Nakanishi, in: *Circular Dichroism. Principles and Applications*, 2nd ed. (Eds.: N. Berova, K. Nakanishi, R. W. Woody), Wiley-VCH, New York, **2000**, pp. 337–382; c) N. Harada, K. Nakanishi, N. Berova, in: *Comprehensive Chiroptical Spectroscopy*, vol. 2 (Eds.: N. Berova, P. L. Polavarapu, K. Nakanishi, R. W. Woody), Wiley-VCH, New York, **2012**, pp. 115–166.
[16] K.-i. Yamashita, K. Kataoka, M. S. Asano, K.-i. Sugiura, *Org. Lett.* **2012**, *14*, 190–193.
[17] G. A. Hembury, V. V. Borovkov, Y. Inoue, *Chem. Rev.* **2008**, *108*, 1–73.
[18] C. Brückner, J. J. Posakony, C. K. Johnson, R. W. Boyle, B. R. James, D. Dolphin, *J. Porphyrins Phthalocyanines* **1998**, *2*, 455–465.
[19] P. J. Angiolillo, V. S. Y. Lin, J. M. Vanderkooi, M. J. Therien, *J. Am. Chem. Soc.* **1995**, *117*, 12514–12527.
[20] R. D. Hartnell, A. J. Edwards, D. P. Arnold, *J. Porphyrins Phthalocyanines* **2002**, *6*, 695–707.
[21] M. O. Senge, X. Feng, *J. Chem. Soc., Perkin Trans. 1* **2000**, 3615–3621.

Received: July 11, 2012
Published Online: October 9, 2012

